

VAPOR COMPRESSION DISTILLER AND MEMBRANE TECHNOLOGY FOR WATER REVITALIZATION

A. Ashida,* K. Mitani,** K. Ebara,*** H. Kurokawa,*** I. Sawada,# H. Kashiwagi,#
T. Tsuji,# S. Hayashi,+ K. Otsubo+ and K. Nitta+

*Planning & Engineering Department, Space Systems Division, Hitachi, Ltd. 4-6 Kanda-Surugadai, Chiyoda-ku, Tokyo 101, Japan, **Satellite Systems Department, Space Systems Division, Hitachi, Ltd., 216 Totsuka-ku, Yokohama 244, Japan, ***Hitachi Research Laboratory, Hitachi, Ltd. 3-1-1 Saiwai-cho, Hitachi 317, Japan, #Sasakura Engineering Co., Ltd. 4-7-32 Takeshima, Nishiyodogawa-ku, Osaka 555, Japan, +National Aerospace Laboratory, 7-44-1 Jindaiji Higashimachi, Chofu, Tokyo 182, Japan.

ABSTRACT

Water revitalization for a space station can consist of membrane filtration processes and a distillation process. Water recycling equipment using membrane filtration processes was manufactured for ground testing. It was assembled using commercially available components. Two systems for the distillation are studied; one is an absorption type thermopervaporation cell and the other is a vapor compression distiller. Absorption type thermopervaporation able to easily produce condensed water under zero gravity was investigated experimentally and through simulated calculation. The vapor compression distiller was studied experimentally and it offers significant energy savings for evaporation of water.

INTRODUCTION

Engineering and experimental studies on water recycling systems for space stations have been conducted by the NAL (National Aerospace Laboratory), Hitachi, Ltd., and the Sasakura Engineering Co., Ltd. The system is applicable to purification of waste water from the crew and from life science experiments in the space station /1/. The equipment for ground-based experiments of a three-step filtration process was manufactured by Hitachi, Ltd. /2/. Two types of distillation under study are presented: the absorption type thermopervaporation membrane evaporation by Hitachi, Ltd. /3/ and vapor compression distillation (VCD) by the Sasakura Engineering Co, Ltd.

The water purification process consists of a three-step filtration involving prefiltration, ultrafiltration and reverse osmosis; activated charcoal removes solutes, such as trace organic materials left in the previous filtration process; and distillation which further purifies water treated through the filtration processes in order to produce potable water. In addition for storing the treated water, an ultraviolet sterilizer is provided to prevent the growth of bacteria.

EQUIPMENT FOR GROUND EXPERIMENTS

To make an optimal system configuration of water revitalization for space stations or in a CELSS, various experiments, especially regarding water quality in each process, should be conducted in order to figure out technical difficulties and to check and confirm maintainability, safety and reliability. For this purpose, equipment for ground experiments for water recycling was manufactured by Hitachi, Ltd. for the NAL. This experimental equipment consists of three-step filtration and the activated charcoal.

The processing performance meets requirements for the IOC Japanese life science missions of an average of 2.1 ℓ of water a day including 0.5 ℓ potable water.

However, the actual performance exceeds these requirements; the processing rate is 10 ℓ /h for ultrafiltration and 0.6 ℓ /h for reverse osmosis, because the components used have higher specifications. The ultra-

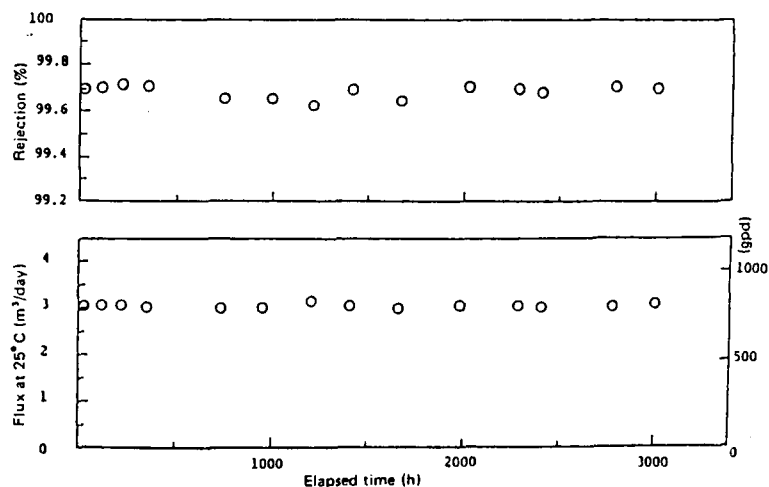


Fig. 1. Brackish water desalination performance of NTR-7199 membrane.

filtration module and the reverse osmosis module were supplied by the Nitto Electric Industrial Co., Ltd. (Ultrafiltration Module: NTU-3250-C1Rc [spiral wound type] and Reverse Osmosis Module: NTR-7199-92Bx [capillary type]). The modules were remodeled from commercial products into products with a smaller processing capability in order to adjust them to the pumps used. Each filtration process has a different processing rate, except the activated charcoal which depends on the permeate rate from the reverse osmosis module, so the system is operated in a batch processing manner.

Experimental studies using this experimental equipment will be made in the near future. Data of a membrane of the same type as the membranes used are shown in Fig. 1, where water flux and salt rejection remained at constant high values throughout the 3000-h test /4/.

ABSORPTION TYPE THERMOPERVAPORATION

The thermopervaporation process uses a hydrophobic membrane of porous polytetrafluoroethylene (PTFE) which was chosen because it permeates vapor, not liquids. This membrane is under development in cooperation with Nitto Electric Industrial Co., Ltd. The permeate flux is proportional to the vapor pressure difference (ΔP) between the feed and the permeated water, expressed by $F = K \cdot \Delta P$, where K is the proportionality constant (permeate coefficient) representing the permeate rate. The electrical conductivity of the treated water is below $10 \mu S/cm$, compared to $48 mS/cm$ of the feed, and the rejection is more than 99.99 %, irrespective of the vapor pressure difference ΔP .

In the former type of thermopervaporation /1/, the problem arose from how to collect the condensed water from the cooled plate in micro gravity. It is easy to collect such water on earth due to the existence of gravity. To resolve this problem the absorption type thermopervaporation is proposed for easy water-gathering, because the permeated vapor is absorbed into the product water. In this system, the feed on the high temperature side of the membrane is vaporized, permeated through the membrane pores, and then absorbed into the cooled permeate which is circulating.

Experimental Study

Experimental data from absorption type is compared to the earlier type process and is shown in Fig. 2, in which black circles show the results of absorption type thermopervaporation corresponding to a diffusion gap of zero.

The value of K is scattered in the range of 1 to $5 \text{ kg/m}^2 \cdot \text{day} \cdot \text{torr}$. This can be explained by the fact that the bulk temperature difference (ΔT) differs from the temperature difference ($\Delta T'$) contributing to the real vapor transfer through the membrane due to the temperature drop near the membrane, as shown in Fig. 2. Moreover, the rate of vapor transfer in the membrane depends on its thickness and porosity. Thus, for the thicker the membranes or the smaller the voids, the more resistant the membrane becomes to the permeate flux. Thus K is affected by the material and structure of the membrane and the operating conditions. From these experimental results, at least $1 \text{ kg/m}^2 \cdot \text{day} \cdot \text{torr}$ was verified. However, in this method, the loss in the sensible heat transfer increases in comparison with the former method. Therefore, further evaluation is needed to reduce this thermal loss.

Theoretical Study

The theoretical study was made based on a model with a heat exchanger (see Fig. 6), which is provided for energy recovery in order to reduce power consumption. Calculations were made concerning the necessary heat input (Q/Q_0), the circulation rate (W) of the feed, the effective heat transfer area (A_{he}), and the effective membrane area (A_m) versus the temperature difference (ΔT) between the feed and cooled water, the temperature difference (ΔT_i) between the inlet and outlet of the feed, and the membrane thickness (δ), where Q_0 is the heat input in case of no heat loss, expressed as $Q_0 = F' \lambda A_m = 0.25 \lambda$ ($F' A_m = 0.25 \text{ kg/h}$, F' : permeate rate, λ : latent heat). ΔT_i is assumed to be the same as for the cooled water, since the circulation rate of the feed is the same as that of the cooled water and the temperature difference in the heat transfer in the heat exchanger is fixed at 5°C . In this calculation, the following parameters are predetermined, thermal conductivity of the membrane = $0.0634 \text{ kcal/mh}^\circ \text{C}$, permeate = 0.25 kg/h , feed water = 0.28 kg/h , concentrate = 0.03 kg/h .

Figs. 3 to 5 show the calculated results. As shown in Fig. 3, ΔT is best when set to 5°C , specifically from the viewpoint of minimum thermal loss. A temperature $T_{lin} = 90^\circ \text{C}$ of the feed at inlet is desirable for efficiency.

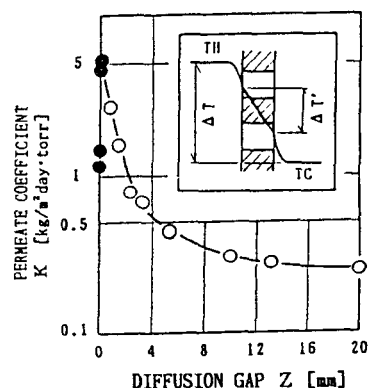


Fig. 2. Experimental results of thermopervaporation

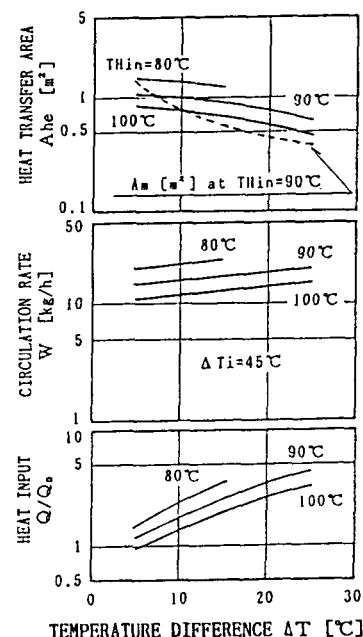


Fig. 3. Influence of ΔT on Q , W and A_{he} .

The diagram shows a distillation column with a reboiler and a condenser. The feed enters at 20 °C and 0.28 g/h. The reboiler heats the feed to 90 °C, and the condenser cools the top product to 20 °C. A heat exchanger preheats the feed from 20 °C to 25 °C. The top product is 0.25 g/h at 20 °C. The bottom product is 0.03 g/h at 25 °C. The reboiler is a vertical vessel with a heating coil. The condenser is a vertical vessel with a cooling coil. The heat exchanger is a horizontal vessel with a heating coil. The feed is pumped from the bottom to the reboiler. The top product is pumped from the condenser to the top of the column. The bottom product is pumped from the reboiler to the bottom of the column. The heat exchanger is located between the feed and the reboiler.

Fig. 6. Suitable conditions of thermopervaporation process

VAPOR COMPRESSION DISTILLATION (VCD)

Principles and Features of VCD

In applying VCD to space stations, artificial gravity is needed for gathering liquids. Fig. 8 shows a concept of a VCD unit to be operated in micro gravity. The inside of the casing is kept at a vacuum by a vacuum pump. The two drums, fixed to each other, and the blower are rotated by the motor. The feed water forms a film on the surface of the inner drum due to centrifugal force and evaporates. The generated vapor in the inner drum is compressed, introduced into the gap between the two drums and then condenses on the inner drum surface, discharging energy for evaporation of the feed. The residual brine and the condensed distillate flows along the tapered drum surfaces and is collected at the troughs.

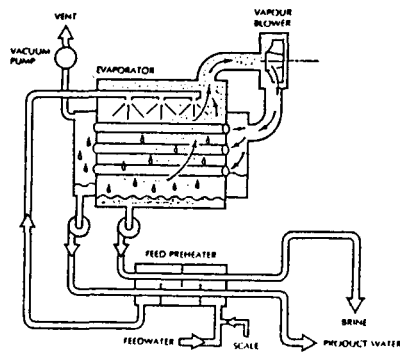


Fig. 7. VCD for seawater desalination

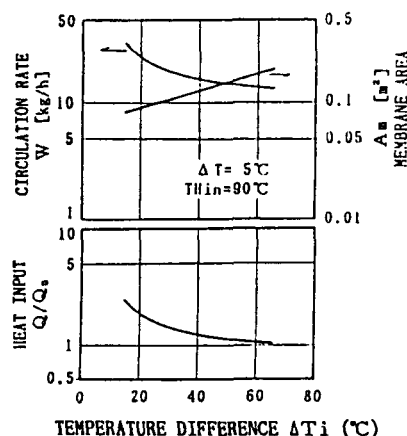


Fig. 4. Influence of ΔT_i on Q , W and A_m

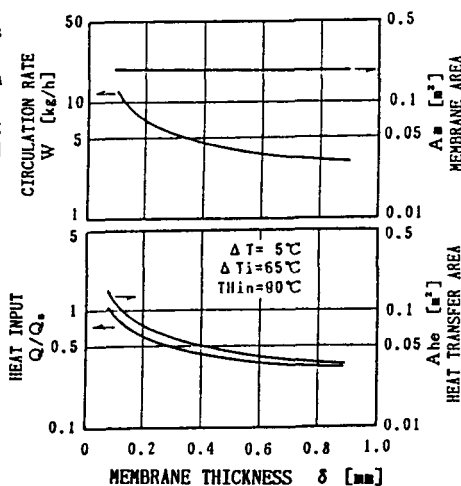


Fig. 5. Influence of δ on Q , W , A_{he} and A_{Σ} .

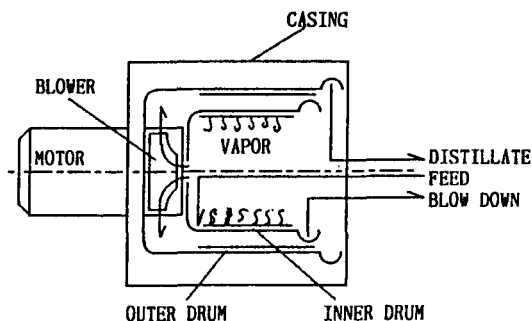


Fig. 8. VCD concept for space use

Experimental Study

An experimental model having a 450 mm diameter and a 620 mm length was made to produce one liter of water per hour, a chart of which is shown in Fig. 9. The feed is preheated in the water bath and the measured amount is sucked by the distiller which is kept in vacuum conditions. The product water and the residual brine are extracted by the twin element pump. The temperature, the pressure and the flow rate are monitored at necessary points. A level alarm is installed in the inner drum to prevent carry over of the feed water to the blower. The distiller employs a single motor for both drum rotation and blower performance.

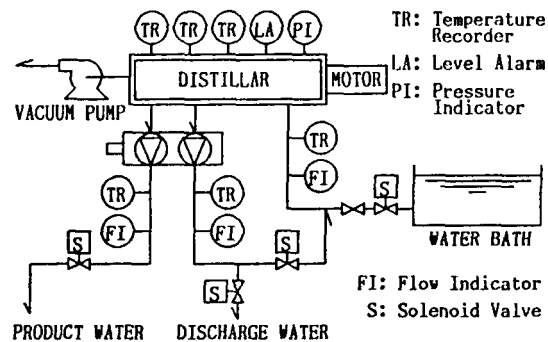


Fig. 9. Flow chart of the experimental VCD model

Fig. 10 shows experimental data of the distillate production rate versus the temperature difference between the blower inlet and outlet (Δ - Δ). The temperature in the inner drum was kept at $29 \pm 0.3^\circ\text{C}$ during this test. The distillate production rate increases as the rotation speed increases, but the rate of increase is a little less than the increase rate of the temperature difference between the inlet and outlet of the blower. It is presumed that the temperature at the outlet of the blower is superheated due to compression and the temperature difference described in Fig. 9 is not the difference of saturation temperature. Another reason would be that the pressure drop through the vapor path becomes large as the distillate production (vapor flow rate) increases, and the actual saturation temperature difference across the heat transfer surface becomes smaller than the superficial temperature difference as the vapor flow rate increases.

Experimental results shown in Fig. 10, (\circ - \circ) in the case of desuperheating, are obtained when desuperheating water is introduced into the suction of the blower. It shows that the relationship between the rate of increase in the distillate production becomes large due to the desuperheating effect.

The evaporation temperature can be controlled by adjusting the feed water temperature. Fig. 11 shows the distillate production and the temperature difference between the blower inlet and outlet versus the evaporation temperature. The distillate increases as the evaporation temperature increases. The reason for this phenomenon is that the heat transfer coefficient increases with increases in the evaporation temperature. Since the temperature difference decreases with elevation of the evaporation temperature, the rate of increase of the heat transfer coefficient is presumed to be of significance. Another reason may be due to a decrease of the pressure drop across the vapor path, in other words, increase in the effective temperature difference across the heat transfer surface due to the increase in the density of the vapor as the temperature increases.

CONCLUSIONS

Water revitalization for the space station can be realized by a combination of the filtration processes and a distillation process. Detailed systematic studies will be performed using ground-based equipment. There are two candidate distillation process; thermopervaporation and VCD. The absorption type thermopervaporation was studied through simulated calculations, so that an optimum condition were obtained. The VCD with centrifugation was experimentally confirmed to be a candidate for space use.

REFERENCES

1. K. Nitta, A. Ashida, K. Mitani, K. Ebara, and A. Yamada, Water recycling system using thermopervaporation method, *CELSS '85 Workshop* NASA TM 88215, January 1986, p. 201.
2. K. Mitani, A. Ashida, K. Ebara, and K. Nitta, Water recycling for space station, 15th ISTS-TOKYO, 1986.
3. K. Ebara, H. Kurokawa, A. Yamada, Y. Koseki, and A. Ashida, Water recycling system using thermopervaporation, 15th ISTS-TOKYO, 1986.
4. Y. Kamiyama, N. Yoshioka, K. Matsui, and K. Nakagome, New thin-film composite reverse osmosis membranes and spiral wound modules, *Desalination*, 51, 79-92 (1984)

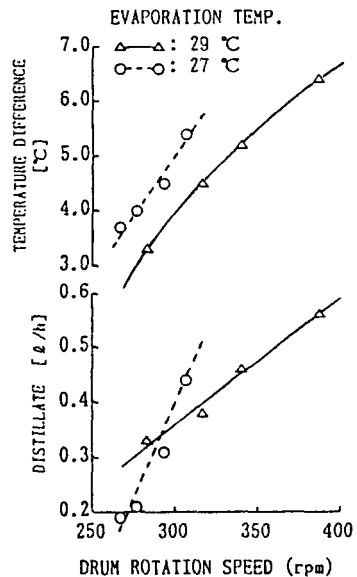


Fig. 10. Effect of drum rotation

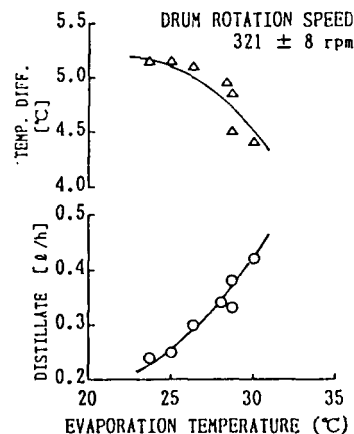


Fig. 11. Dependence of distillate and temperature difference on evaporation temperature.